ECOLOGY

Twentieth century redistribution in climatic drivers of global tree growth

Flurin Babst[1,2,3]*, Olivier Bouriaud[4], Benjamin Poulter[5], Valerie Trouet[3], Martin P. Girardin[6,7], David C. Frank[1,3]

Energy and water limitations of tree growth remain insufficiently understood at large spatiotemporal scales, hindering model representation of interannual or longer-term ecosystem processes. By assessing and statistically scaling the climatic drivers from 2710 tree-ring sites, we identified the boreal and temperate land areas where tree growth during 1930–1960 CE responded positively to temperature (20.8 ± 3.7 Mio km^2; 25.9 ± 4.6%), precipitation (77.5 ± 3.3 Mio km^2; 96.4 ± 4.1%), and other parameters. The spatial manifestation of this climate response is determined by latitudinal and altitudinal temperature gradients, indicating that warming leads to geographic shifts in growth limitations. We observed a significant ($P < 0.001$) decrease in temperature response at cold-dry sites between 1930–1960 and 1960–1990 CE, and the total temperature-limited area shrunk by −8.7 ± 0.6 Mio km^2. Simultaneously, trees became more limited by atmospheric water demand almost worldwide. These changes occurred under mild warming, and we expect that continued climate change will trigger a major redistribution in growth responses to climate.

INTRODUCTION

Global variations in plant growth have been attributed to interactions between temperature, precipitation, and radiation budgets (1–3), rather than to a single driver, as suggested by Liebig's law of the minimum. Basic physiological processes such as photosynthesis and cell division are tempered where plant-available energy and water are low. With increasing energy inputs, water availability often becomes the primary limitation of plant growth. Understanding this interplay between energy and water effects is thus essential to anticipate climate change impacts on the combined biogeochemical and energy cycles and to quantify their feedbacks within the climate system (4, 5).

Climate affects plants on two interlinked levels that are mediated by plant hydraulics (6): the leaf level, where fast carbon assimilation processes happen, and the stem-root continuum, where carbohydrates are allocated to biomass growth and reserve pools (7). The net results of leaf-level processes can be reasonably well assessed at global scales from observations of canopy dynamics and CO_2 exchange that indicate spatially complex interactions of temperature and water constraints (1–3). By contrast, the relative importance and spatial manifestation of the climatic drivers of plant growth are uncertain. This is because growth observations that are geographically extensive and, at the same time, cover long time scales remain scarce. This shortage particularly concerns trees and shrubs, whose longevity exceeds the length of existing Earth observation records (8). Hence, tree growth and its drivers need to be assessed from in situ observations. Climate is thereby not the only relevant force, and tree size, age, and competition are also important determinants of biomass changes in forests (9, 10). Still, energy and water availability and demand are the drivers that are projected to dramatically change in the future (4) and that will potentially seriously affect the growth trajectories of forest ecosystems (11, 12).

The structure and parameterization of global vegetation models (GVMs) reflect this discrepancy in our understanding of what limits carbon uptake and biomass growth of trees. GVM predictions are primarily driven by photosynthesis, and their parameterization is based on temporally highly resolved but short-term observations from eddy covariance and remote-sensing systems or from laboratory experiments (13, 14). Accordingly, GVMs are capable of simulating short-term forest carbon uptake with precision, whereas annual or longer-term ecosystem processes are insufficiently represented (13, 15–17). This problem is evidenced by model-data discrepancies (12, 15–20) and the considerable spread in the annual climate sensitivity of current GVM ensembles (4). Refined carbon allocation schemes (21), as well as better representation of growth processes and their climate response in GVMs, have been highlighted as a way to improve the models and refine projections of the forest carbon balance (13, 18–20). Yet, like any model representation of biophysical processes, this approach should be well grounded in large-scale observations.

In this study, we aim to provide the missing empirical baseline of how tree growth responds to climate variability across temperate and boreal forest biomes. To reach this unprecedented spatial scale, we leveraged a global network of cross-dated tree-ring width data from 2710 sites (fig. S1) and calculated single-species site chronologies (see Materials and Methods). At each site, we quantified the response of interannual variability in tree growth to four climate parameters (subsequently called "climate response") during 1930–1960 and 1960–1990 CE (see Materials and Methods). These parameters were used as metrics of energy [temperature (T)] and water [precipitation (P) availability, atmospheric water demand [vapor pressure deficit (VPD)], and drought [standardized precipitation evapotranspiration index (SPEI)]. Energy-limited trees are expected to respond positively to T, whereas water-limited trees will respond positively to P and SPEI and negatively to VPD (11, 12, 15, 18–20). We then performed two steps of generalization. First, we grouped the site-level climate response using affinity propagation clustering (22) to identify the relevant seasons for tree growth in different climatic domains. Second, we interpolated the site-level climate response across the climate envelope that encompasses 99% of the sites (i.e., to minimize edge effects from climatic domains with low tree-ring representation). The resulting trend surfaces allowed us to map the climate response of trees geographically based on the

[1]Dendro Sciences Group, Swiss Federal Research Institute WSL, Zürcherstrasse 111, CH-8903 Birmensdorf, Switzerland. [2]Department of Ecology, W. Szafer Institute of Botany, Polish Academy of Sciences, ul. Lubicz 46, 31-512 Kraków, Poland. [3]Laboratory of Tree-Ring Research, University of Arizona, 1215 E. Lowell St., Tucson, AZ 85721, USA. [4]Stefan cel Mare University of Suceava, Strada Universității 13, Suceava 720229, Romania. [5]NASA Goddard Space Flight Center, Greenbelt, MD 20771, USA. [6]Laurentian Forestry Centre, Canadian Forest Service, Natural Resources Canada, Quebec, QC G1V4C7, Canada. [7]Centre d'étude de la forêt, Université du Québec à Montréal, C.P. 8888, succ. Centre-ville, Montréal, QC H3C 3P8, Canada.
*Corresponding author. Email: flurin.babst@wsl.ch

growing season temperature (see fig. S2 for definition) and annual precipitation of each grid cell. The results from these two steps of generalization were then assessed to (i) identify the importance and seasonality of the four climate parameters for tree growth around the globe and (ii) test for shifts in the climate response of trees between the mid (1930–1960) and late (1960–1990) 20th century.

RESULTS

The first step of generalization clustered the sites into four distinct groups that correspond to cold-humid, hot-dry, cold-dry, and temperate climatic domains (Fig. 1). This distinction emerged solely from the monthly to seasonal climate response, without considering any information on site climate or geographic location. We find a strong seasonality in the growth response to T and VPD (Fig. 2, A and C). For example, significant positive and negative correlations with summer T in cold-humid and hot-dry areas, respectively, indicate that T was an important driver of growth rates between 1930 and 1960 CE [cluster mean $P < 0.001$, assessed using Fisher's method; (23)]. In addition, significantly positive T responses in spring and previous autumn in temperate and cold-humid areas, respectively, suggest that trees can benefit from a long growing season. In contrast to T-driven metrics, the seasonality in the growth response to P and SPEI is much less pronounced (Fig. 2, B and D). In cold-humid, hot-dry, and temperate domains, trees respond to the integrated water availability over the previous and current years, rather than during individual seasons.

The spatial interpolation of the climate response in the second step of generalization (Fig. 3) covers the contemporary climate envelope of −1.7° to +25.8°C growing season temperature and 157 to 2908 mm an-

nual precipitation. This translates into a geographic coverage of 55.2% of the global land surface and 69.9% of the present-day global forest area (fig. S1). The tree-ring sites are reasonably well distributed within this climate envelope, but data availability becomes sparser toward the edge, particularly in warm-humid domains. Accordingly, the uncertainty associated with the spatial interpolation is larger in these climates (Fig. 3C) that are mostly prevalent in subtropical regions of Africa, South America, and Indonesia (fig. S3). When the interpolated climate response is projected into geographic space, it becomes evident that the area where trees are primarily energy limited and respond positively to T is restricted to cold and humid regions in southern Alaska, northeastern Canada, coastal Scandinavia, the Alps, Tibet, and northeastern Siberia (Fig. 4A). We quantified this area at 20.8 ± 3.7 Mio km² for 1930–1960 CE (Table 1). By contrast, moisture-limited trees that respond positively to water availability and negatively to drought and atmospheric water demand can be found across the globe (i.e., across 96.4 ± 4.1% of the represented land area in the case of P). The strongest water limitation thereby occurs in the lower to mid latitudes (Fig. 4, B to D, and fig. S5). Overall, the spatial manifestation of climate response was dominated by latitudinal and altitudinal T gradients. Linear models showed that growing season temperature explained between 52 and 79% of the variance (depending on the climate parameter) in the interpolated climate response between grid cells, whereas annual precipitation explained almost none (table S1). This result indicates that changes in baseline T—such as the warming that is projected for the 21st century (4)—will alter the geographic distribution of climate response, with likely effects on tree growth rates (11, 12) and maybe even the potential to trigger biome shifts (24, 25).

The observation that global warming can trigger geographic shifts in climate response leads to the question of whether these shifts have
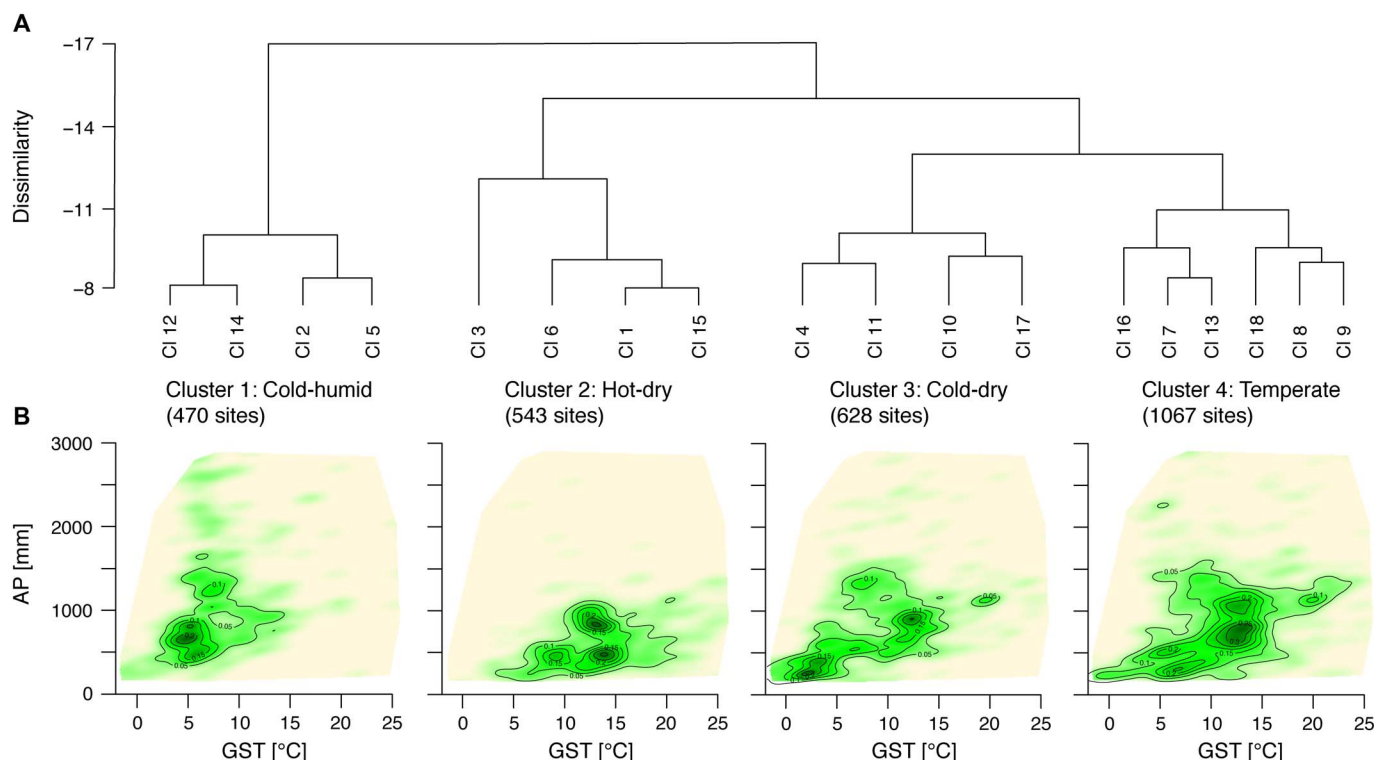

Fig. 1. The 2710 sites that constitute the tree-ring network are assigned to four main clusters based on their monthly to seasonal climate response. These four clusters consist of 18 subclusters (**A**) and correspond to cold-humid, hot-dry, cold-dry, and temperate domains (**B**). GST, growing season temperature; AP, annual precipitation.
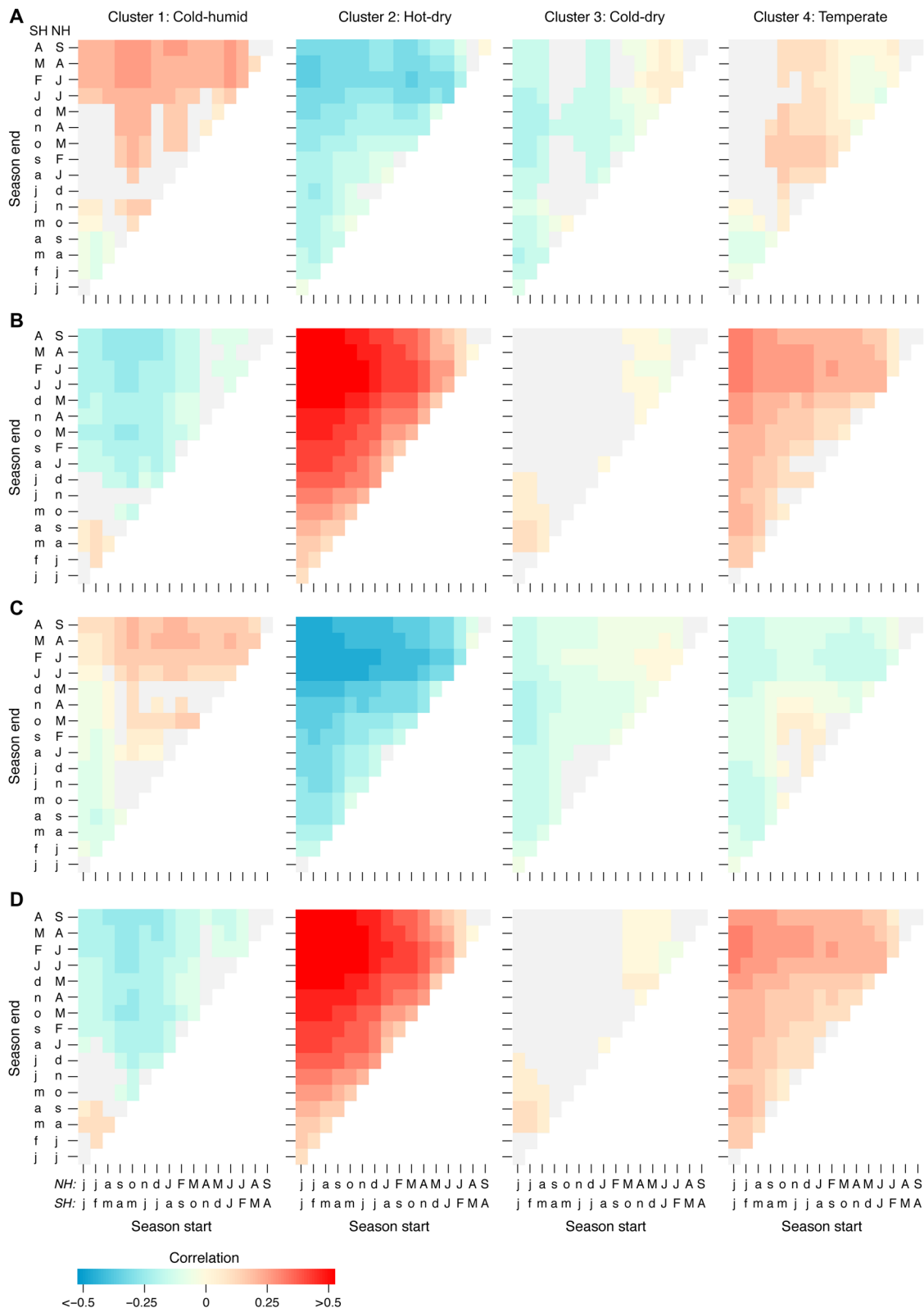
Fig. 2. Climate response of tree growth across the four main climatic domains between 1930 and 1960 CE. For each of the identified domains (see Fig. 1), we present the mean correlations between tree growth and temperature (**A**), precipitation (**B**), VPD (**C**), and the SPEI (**D**). The correlations for individual months are shown on the diagonal, whereas consecutive seasons starting in a given month extend upward. Corresponding partial correlations that show similar patterns are provided in data S1. Gray shading indicates correlations that were not significant ($P > 0.001$) after integrating P values from all sites within a cluster using Fisher's method (23). Small and capital letters refer to the previous and current years. NH, Northern Hemisphere; SH, Southern Hemisphere.
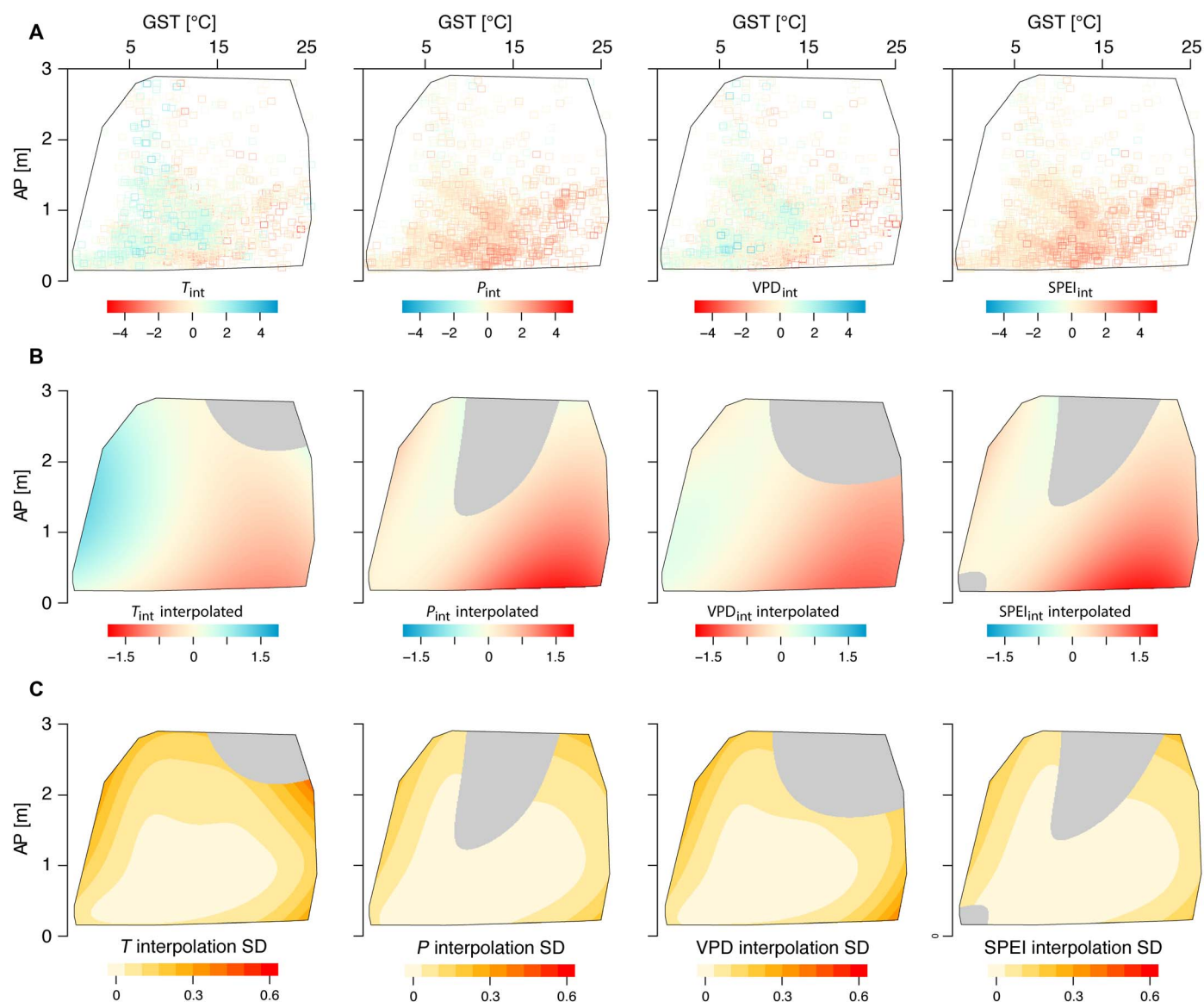
Fig. 3. Spatial interpolation of the climate response from 2710 sites between 1930 and 1960 CE. One value per site was calculated for each climate parameter by integrating the significant ($P < 0.1$) monthly correlations (int) (**A**). This climate response was spatially interpolated within the growing season temperature and annual precipitation envelope of the network (**B**). The uncertainty of the interpolation, as expressed by the bootstrapped SDs from 1000 random network subsets (see Materials and Methods), is shown in (**C**). Please note that the color scale for *P* and the SPEI have been inverted compared with *T* and VPD, so red colors consistently indicate water limitation. Gray shading indicates nonsignificant ($P > 0.1$) areas.

already occurred under the relatively mild warming of the 20th century. Between 1930–1960 and 1960–1990 CE, the four main climate response types that emerged from the clustering (Fig. 1) experienced changes in monthly *T* and *P* of −0.99° to +1.15°C and −15.01 to +12.54 mm (data S2), respectively, with the strongest warming occurring in cold-humid areas. A comparison of the climate responses between these two periods indicates significant changes (two-tailed Student's *t* test with preceding Fisher's *z* transformation to ensure normality, $P < 0.001$) that occurred in different seasons, depending on the climatic domain. In hot-dry areas, trees became more limited by winter and spring precipitation and drought (fig. S5, B and D), which is likely a result of the increasingly discontinuous snow cover in arid mountain ranges, such as in the U.S. Southwest

(*26*). In cold-dry regions, the response to winter *T* became negative toward the late 20th century. During spring, trees benefited from warmer temperatures in both cold-humid and temperate regions (fig. S5A), suggesting that an earlier start of the growing season stimulated tree growth in these domains. During the summer months, limitations imposed by drought and atmospheric water demand increasingly hampered tree growth in cold-humid, hot-dry, and temperate areas (fig. S5, C and D). These combined results imply that climate change during the 20th century has affected trees by altering both the duration (i.e., phenology) and the rate of growth.

Changes in climate response between 1930–1960 and 1960–1990 CE also emerge spatially, with a decrease in energy limitation and a moderate increase in water limitation across the boreal zone and
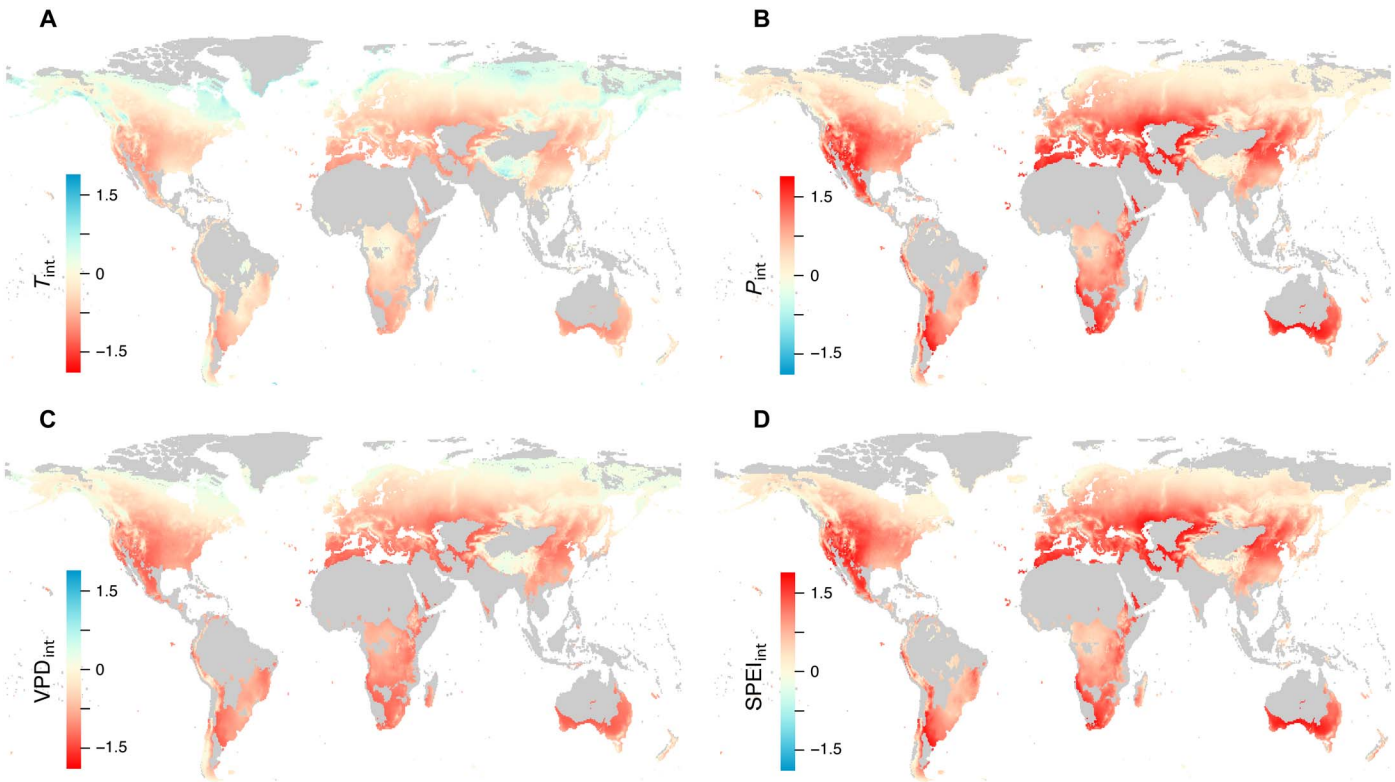
Fig. 4. Geographic distribution of the climate response of tree growth between 1930 and 1960 CE. The maps were produced by projecting the interpolated growth response to (**A**) temperature (T_{int}), (**B**) precipitation (P_{int}), (**C**) vapor pressure deficit (VPD_{int}), and (**D**) standardized precipitation evapotranspiration index ($SPEI_{int}$) from 2710 sites into geographic space based on the growing season temperature and annual precipitation of each grid cell (see Fig. 3). Red colors indicate stronger water than energy constraints; blue colors indicate the opposite. Gray areas fall outside the climate envelope covered by the tree-ring network.

Table 1. The land area where tree growth responded significantly ($P < 0.1$) to different climate parameters has changed between 1930–1960 and 1960–1990 CE. The most pronounced changes occurred for areas that respond positively to temperature ($T_{int} > 0$) and negatively to atmospheric water demand ($VPD_{int} < 0$). By contrast, the responses to precipitation ($P_{int} > 0$) and the standardized precipitation evapotranspiration index ($SPEI_{int} > 0$) remained relatively stable. Δ is the change between 1930–1960 and 1960–1990 CE. The total land area that falls within the climate envelope of the tree-ring network is 80.4 Mio km².

Time	Area	$T_{int} > 0$	$P_{int} > 0$	$VPD_{int} < 0$	$SPEI_{int} > 0$
1930–1960	Mio km²	20.8 ± 3.7	77.5 ± 3.3	66.0 ± 1.6	78.0 ± 1.3
	%	25.9 ± 4.6	96.4 ± 4.1	82.0 ± 2.0	97.0 ± 1.6
1960–1990	Mio km²	12.1 ± 3.1	77.4 ± 0.8	74.7 ± 1.7	77.4 ± 0.8
	%	15.1 ± 3.9	96.2 ± 1.0	92.8 ± 2.1	96.2 ± 1.0
Δ	Mio km²	−8.7 ± 0.6	−0.1 ± 2.6	8.7 ± 0.1	−0.6 ± 0.5
	%	−10.8 ± 0.7	−0.2 ± 3.2	10.8 ± 0.2	−0.8 ± 0.6

in cold-dry regions of Central Asia (fig. S6, A and B). Accordingly, the probability of energy limitation in these regions has weakened, and the importance of water limitation on tree growth has strengthened (Fig. 5). At the same time, trees are increasingly limited by atmospheric water demand (VPD; fig. S6C) in most regions, except in warm-humid

areas in the southeastern United States, Central Africa, the Amazon, and southeastern Asia. When averaged across the globe, the shifts in climate response from energy limitation toward water limitation were significant (two-tailed Student's t test, $P < 0.001$) for T, VPD, and P, but not for SPEI. The represented land area where tree growth is T-limited decreased by $−8.7 ± 0.6$ Mio km² ($−10.8 ± 0.7\%$ of the total area); the area where growth is negatively affected by VPD increased by $8.7 ± 0.1$ Mio km² ($10.8 ± 0.2\%$ of the total area); and the areas where tree growth is water limited, as reflected by the responses to P and SPEI, remained relatively stable between 1930–1960 and 1960–1990 CE (Table 1). These results suggest that rising temperatures and the associated increase in atmospheric water demand have been the main drivers of changes from energy limitation toward water limitation of tree growth in the boreal and temperate zones during the 20th century.

DISCUSSION

This large-scale study demonstrates that the relatively mild shift in baseline climate over the 20th century has already triggered observable changes in the climate response of temperate and boreal tree growth. We find that water availability has replaced energy as the dominant limiting factor across large portions of the boreal zone (Fig. 5), which generalizes in situ observations of diminishing T constraints on boreal tree growth (11, 25, 27, 28). This trend is projected to continue with the 21st century warming (11, 29). Together with the growing atmospheric water demand that can lead to reduced transport of sugars from the leaves to the stem (6, 24, 30), this evidence suggests that drought is
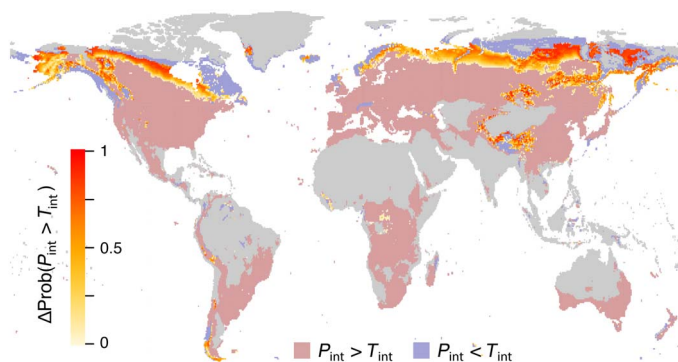
Fig. 5. The probability that precipitation exceeded temperature as the main driver of tree growth has increased throughout the boreal zone between 1930–1960 and 1960–1990 CE. The most pronounced changes (orange to red colors) occurred across cold-dry regions in Alaska, Canada, Finland, and Russia. Accordingly, the area where the temperature response (T_{int}) exceeded the precipitation response (P_{int}) of tree growth, i.e., the blue area on the map, was reduced to cold-humid Alpine and coastal areas, as well as the northernmost taiga in Siberia.

becoming the dominant limitation of tree growth worldwide (fig. S6, C and D). In hot-dry areas, drought is generally associated with lower hydraulic conductivity, reduced photosynthetic carbon uptake, and increased tree mortality (24, 31). However, the extent to which these mechanisms also threaten trees across the temperate and boreal zones will greatly depend on the rate of warming. This adds weight to our finding that the spatial distribution of climate response around the globe mainly follows temperature gradients and not precipitation gradients (table S1). A recent global assessment of the climatic drivers of gas exchange between the forest canopy and the atmosphere drew similar conclusions: Gross primary productivity (GPP) and ecosystem respiration, both mainly controlled by water availability at the site level, compensate each other to leave a dominant T signal in the global variations in net ecosystem exchange (3). Yet, across the boreal zone where recent canopy greening has largely been attributed to warming (32), we observe a comparatively weak growth response to T (Fig. 4). This is likely because trees can access carbohydrate reserves to sustain growth, leading to lag effects that are evidenced by significant correlations with previous year's climate (Fig. 2). Hence, the climate response of tree growth is less instantaneous compared with that of photosynthesis (7, 15–20). Carbohydrate reserves are now starting to be implemented in GVMs, and our global climate response maps can serve as independent benchmarks for the climate response simulated with refined carbon allocation schemes (21).

We note that our tree-ring network does not provide quantitative information on forest growth because tree biometric and stand-level data (stand density, tree size distribution, forest dynamics, and mortality) are missing for most sites. We also acknowledge that the tropics are underrepresented in our tree-ring network and that the distribution of sites is biased toward Europe and North America (8), which was our main incentive for performing the spatial interpolations in climatic space and not in geographic space. This analysis was done under the assumption that biogeographic patterns in climate response are much stronger than species-specific differences. This is yet to be tested at global scales, but a recent study at least indicated that several species-specific traits across eastern North America were poor predictors of drought sensitivity (33). We also presume that the climate response derived from tree-ring records is relatively insensitive to variations in sampling protocols (34).

A potential concern for this large-scale study was that the climate response of the tree-ring network could be inflated [i.e., a "climate sensitivity bias"; (35)] because a subset of sites was specifically sampled to maximize their sensitivity to a single parameter for climate reconstruction. To address this concern, we performed linear regression and analysis of covariance (ANCOVA), comparing the climate response of our network to that of two independent reference networks. These networks were collected within Canada's systematic national forest inventory (36) and within a European initiative to quantify historical forest biomass increment for carbon accounting and GVM evaluation (37) (data S3). As data collection was guided by ecological and spatial questions, rather than paleoclimatological principles, their representativeness for forests should be much improved compared with that of the International Tree-Ring Data Bank (ITRDB). Trees in the Canadian and European networks are also younger (97 and 92 years, on average) and thus closer to the average forest age compared with the mean series length of 195 years in our network. Our analyses showed a similar climate response among the three networks (see Materials and Methods, fig. S7, and table S2). Hence, while parts of our dataset are likely subject to the climate sensitivity bias, the climate response of the overall network appears not to be much enhanced, allowing us to have confidence in the observed spatiotemporal patterns.

The most pronounced changes in climate response occurred in the boreal zone, where decreasing T controls on canopy greenness have also been reported (1). Boreal tree populations are adapted to cold environments, which reduces their responsiveness to T variability (38). Hence, the observed shifts are likely amplified by long generation times that prevent forests from adapting quickly to changing environmental conditions. Predicted 21st century warming (4) is expected to further accelerate this redistribution of climatic drivers and, in particular, to strengthen atmospheric water demand as a primary determinant of large-scale changes in tree growth (11, 39). Rising atmospheric CO_2 concentrations may partly alleviate this drought stress because they will cause for more carbon to be sequestered per unit of water loss, but the magnitude and persistence of this carbon fertilization effect remain under debate (11, 19, 36). Climate change impacts on forests range from increased growth in cold-humid environments to enhanced risk of widespread tree mortality in drought-prone areas (11, 24, 25, 27, 28), reinforcing the need for improved silvicultural countermeasures (40). Refined projections of the associated changes in the terrestrial carbon balance are needed to support climate change decision-making (4, 5). Our empirical assessment of the long-term and large-scale climate response of tree growth can support this process by informing GVMs, the major forecasting tool that still struggles to precisely and accurately reflect annual to longer-term growth responses to climate (4, 12–21).

MATERIALS AND METHODS
Experimental design
We homogenized a tree-ring width network comprising 2337 single-species records from the ITRDB and 373 records from (18). Quality criteria for the retained chronologies included a minimum sample replication of five trees, significant ($P < 0.05$) mean correlations between the constituting tree-level measurements, and full coverage of the 1930–1990 CE period. The network includes 213 species (78.5% gymnosperms and 21.5% angiosperms), 50% of which belong to the genera *Pinus*, *Picea*, and *Quercus*. The age/size-related trends in the raw data were removed from all series using cubic smoothing spline detrending with a 50% frequency cutoff at 30 years. The heteroscedastic variance structure was

stabilized using adaptive power transformation prior to detrending. This procedure preserved interannual growth variability in the resulting tree-ring indices while removing long-term trends. The detrended tree-level series were averaged into site-level chronologies using a biweight robust mean. We estimated a common growing season for all sites based on the monthly course of GPP from 51 forested FLUXNET2015 sites that offer more than 5 years of data (Tier 1 data only; see data S4). These sites represent the temperature domain covered by the tree-ring network well (fig. S2A) and indicate a growing season between April and October (between October and April) for the Northern (Southern) Hemisphere when GPP is markedly positive (fig. S2B).

It has been hypothesized that the climate sensitivity of the ITRDB could be inflated because a subset of sites has been sampled for dendroclimatic purposes (35). To evaluate this possible bias with respect to our study, we obtained two independent tree-ring datasets from Canada's National Forest Inventory (36) and from a European biomass network [(37); data S3] and detrended them in the same way as our global network. These reference datasets have not been collected for dendroclimatological purposes, and we used them to benchmark ITRDB's climate sensitivity. We found that (i) the scatter of the three networks overlaps greatly, indicating that the ITRDB is not a marginal sample (fig. S7); (ii) ITRDB was not the most climate sensitive of the three networks; and (iii) effects of "dataset" in a series of ANCOVA analyses were mostly insignificant (table S2). Hence, we consider our tree-ring network to be suitable for the purpose of this study.

Statistical analyses
Climatic drivers of growth interannual variability
We assessed the climatic drivers at each site during two 30-year periods between 1930–1960 and 1960–1990 CE. Prior to 1930, the quality of the used CRU-TS3.21 climate dataset (41) was insufficient at 301 remote sites in boreal North America and Asia and in South America. After 1990, the decrease in available tree-ring data toward the present (8) critically reduced the covered space. We obtained four gridded monthly climate parameters from CRU-TS3.21: T, P, VPD, and SPEI. VPD was calculated as saturated minus actual vapor pressure, and SPEI was calculated using the R package "SPEI" (42). We calculated regular and partial (data S1) Pearson correlation coefficients between the detrended tree-ring chronologies and monthly to seasonal climate from the corresponding CRU-TS3.21 grid cell over a 16-month window between previous June (January) and current September (April) for the Northern (Southern) Hemisphere. This window was chosen to account for potential 1-year lag effects in the climate response (11, 18, 20).

In a first step of generalization, the relevant climatic seasons for interannual growth variability were identified using affinity propagation clustering (22) that included the site-level correlations over all months and consecutive seasons. This "message-passing" algorithm independently selects exemplary sites, without a predefined number of clusters. We set the "input preference" (the tendency of sites to become exemplars) to the lowest quantile to achieve maximum generalization. This analysis yielded 18 clusters that group into four distinct climate response types (Fig. 1). Correlations from all sites within each group were averaged, and their significance levels were assessed using Fisher's method (23).

Projection of climate response into space
In a second step of generalization, we projected the site-level climate response into growing season T and annual P space to achieve continuous coverage of the climatic domains occupied by extratropical forests. Problematically, the 0.5° spatial resolution of CRU-TS3.21 resulted in coarse representation of site climate, particularly in steep terrain. To correctly place sites in climate space, we obtained the long-term mean (1950–2000 CE) monthly T and P data for each site from the WorldClim database (43) at 1-km resolution. The monthly T and P data from CRU-TS3.21 were scaled to WorldClim over 1950–2000 CE before calculating growing season T and annual P for both 30-year periods.

Our cluster analysis (see above) showed no single season that explained interannual growth variability at global scales. Hence, to further generalize the diverse site-level climatic drivers for upscaling, we adapted an integrative approach (11) that targets the overall climate response and averages out seasonal responses that can have opposite signs (observed at 38% of sites). The monthly correlations were summarized as

$$\text{clim}_{\text{int}} = \sum_{i=1}^{n} \text{corr}(\text{TRW}, \text{clim}_i)$$

where clim_{int} is the growth response to the respective climate parameter over n significant ($P < 0.1$) months [integrated using Fisher's method (23)], i is the focal month, TRW is detrended tree-ring width, and clim is the focal climate parameter.

Site-level clim_{int} were interpolated using a third-order polynomial trend surface that included site elevation as an additional predictor (see custom code in data S5). We chose this relatively rigid interpolation over locally driven (e.g., spline) approaches to reduce potential biases originating from the fact that the ITRDB is not a systematic sample of forest biomes (8, 35). Extracting the interpolated clim_{int} for each grid cell based on its growing season T and annual P produced continuous climate response maps.

Uncertainty of the spatial interpolation
We evaluated the spatial interpolation in several steps: (i) We examined the sample experimental variogram for directional biases related to growing season T or annual P in the spatial autocorrelation. No such biases were observed. (ii) We tested the residuals of linear models between observed and interpolated clim_{int} values for dependency on climate or geographic parameters (latitude, longitude, and elevation). No significant relationships ($P < 0.1$) were found. (iii) We adopted a Monte Carlo approach and selected random subsets of the tree-ring network, thereby iteratively decreasing the number of sites by 5%. For each step, we sampled the tree-ring network and performed the spatial interpolation 1000 times (with replacement), reporting their bootstrapped means and SDs as uncertainty (Fig. 3C and fig. S3). In addition, we compared the clim_{int} distribution at each step with the distribution of the interpolation based on the full network (Kolmogorov-Smirnov test). Significant differences ($P < 0.1$) were not found before the network replication dropped below 60%. (iv) We performed the spatial interpolation on the basis of geographic subsets and compared the results to those obtained from the full network (table S3). The number of sites ($n = 874$) and the represented climate space (3.8° to 21.4°C growing season T; 226- to 2265-mm annual P) were the smallest for Europe. Hence, we restricted the analysis to this climate space, where 1182 sites from North America and 2509 sites from the full network fell. We selected random subsets ($n = 874$) from North America and the full network 1000 times with replacement. The means of these 1000 runs were used in the linear models presented in the upper half of table S3. (v) We performed the spatial interpolation based on climate space subsets and compared the results to those obtained from the full network (table S3, lower half). For this purpose, the climate space of the full network was divided into four subsets with above- and below-median growing season T and annual

P: warm-dry (WD; 511 sites), warm-wet (WW; 807 sites), cold-dry (CD; 826 sites), and cold-wet (CW; 510 sites).

SUPPLEMENTARY MATERIALS

Supplementary material for this article is available at http://advances.sciencemag.org/cgi/content/full/5/1/eaat4313/DC1

Fig. S1. Geographic coverage of the tree-ring network.
Fig. S2. Definition of the growing season across the tree-ring network.
Fig. S3. Geographic distribution of the uncertainty associated with the spatial interpolation of climate response.
Fig. S4. Latitudinal changes in the climate response of forest growth during 1930–1960 CE.
Fig. S5. The climate response of tree growth across the four main climatic domains has changed between 1930–1960 and 1960–1990 CE.
Fig. S6. Spatiotemporal changes in the climate response of tree growth between 1930–1960 and 1960–1990 CE.
Fig. S7. Comparison of the summer climate response of three independent tree-ring networks.
Table S1. Relationships between the climate response of tree growth and mean climatic conditions.
Table S2. Comparison of the climate sensitivity of three independent tree-ring networks.
Table S3. Comparison of the interpolated climate response based on the full tree-ring network versus subsets thereof.
Data S1. Partial_correlations_clusters.xlsx.
Data S2. Climate_change_monthly.xlsx.
Data S3. EUR_biomass_network.xlsx.
Data S4. FLUXNET2015_Sites.xlsx.
Data S5. Custom_Code.R.

REFERENCES AND NOTES

1. S. Piao, H. Nan, C. Huntingford, P. Ciais, P. Friedlingstein, S. Sitch, S. Peng, A. Ahlström, J. G. Canadell, N. Cong, S. Levis, P. E. Levy, L. Liu, M. R. Lomas, J. Mao, R. B. Myneni, P. Peylin, B. Poulter, X. Shi, G. Yin, N. Viovy, T. Wang, X. Wang, S. Zaehle, N. Zeng, Z. Zeng, A. Chen, Evidence for a weakening relationship between interannual temperature variability and northern vegetation activity. *Nat. Commun.* **5**, 5018 (2014).
2. A. W. R. Seddon, M. Macias-Fauria, P. R. Long, D. Benz, K. J. Willis, Sensitivity of global terrestrial ecosystems to climate variability. *Nature* **531**, 229–232 (2016).
3. M. Jung, M. Reichstein, C. R. Schwalm, C. Huntingford, S. Sitch, A. Ahlström, A. Arneth, G. Camps-Valls, P. Ciais, P. Friedlingstein, F. Gans, K. Ichii, A. K. Jain, E. Kato, D. Papale, B. Poulter, B. Raduly, C. Rödenbeck, G. Tramontana, N. Viovy, Y.-P. Wang, U. Weber, S. Zaehle, N. Zeng, Compensatory water effects link yearly global land CO₂ sink to temperature. *Nature* **541**, 516–520 (2017).
4. P. Ciais, S. Chris, B. Govindasamy, L. Bopp, V. Brovkin, J. Canadell, A. Chhabra, R. Defries, J. Galloway, M. Heimann, Carbon and other biogeochemical cycles, in *Climate Change 2013: The Physical Science Basis. Contribution of Working Group I to the Fifth Assessment Report of the Intergovernmental Panel on Climate Change*, T. F. Stocker, D. Qin, G.-K. Plattner, M. Tignor, S. K. Allen, J. Boschung, A. Nauels, Y. Xia, V. Bex, P. M. Midgley, Eds. (Cambridge Univ. Press, 2013), pp. 465–570.
5. J. Marotzke, C. Jakob, S. Bony, P. A. Dirmeyer, P. A. O'Gorman, E. Hawkins, S. Perkins-Kirkpatrick, C. L. Quéré, S. Nowicki, K. Paulavets, S. I. Seneviratne, B. Stevens, M. Tuma, Climate research must sharpen its view. *Nat. Clim. Chang.* **7**, 89–91 (2017).
6. L. Sack, M. C. Ball, C. Brodersen, S. D. Davis, D. L. Des Marais, L. A. Donovan, T. J. Givnish, U. G. Hacke, T. Huxman, S. Jansen, A. L. Jacobsen, D. M. Johnson, G. W. Koch, C. Maurel, K. A. McCulloh, N. G. McDowell, A. McElrone, F. C. Meinzer, P. J. Melcher, G. North, M. Pellegrini, W. T. Pockman, R. Brandon Pratt, A. Sala, L. S. Santiago, J. A. Savage, J. Scoffoni, S. Sevanto, J. Sperry, S. D. Tyerman, D. Way, N. Michele Holbrook, Plant hydraulics as a central hub integrating plant and ecosystem function: meeting report for "Emerging Frontiers in Plant Hydraulics" (Washington, DC, May 2015). *Plant Cell Env.* **39**, 2085–2094 (2016).
7. C. M. Litton, J. W. Raich, M. G. Ryan, Carbon allocation in forest ecosystems. *Glob. Chang. Biol.* **13**, 2089–2109 (2007).
8. F. Babst, B. Poulter, P. Bodesheim, M. D. Mahecha, D. C. Frank, Improved tree-ring archives will support earth system science. *Nat. Ecol. Evol.* **1**, 0008 (2017).
9. S. E. Russo, S. K. Wiser, D. A. Coomes, Growth-size scaling relationships of woody plant species differ from predictions of the metabolic ecology model. *Ecol. Lett.* **10**, 889–901 (2007).
10. C. Körner, A matter of tree longevity. *Science* **355**, 130–131 (2017).
11. N. D. Charney, F. Babst, B. Poulter, S. Record, V. M. Trouet, D. Frank, B. J. Enquist, M. E. K. Evans, Observed forest sensitivity to climate implies large changes in 21st century North American forest growth. *Ecol. Lett.* **19**, 1119–1128 (2016).
12. S. Tei, A. Sugimoto, H. Yonenobu, Y. Matsuura, A. Osawa, H. Sato, J. Fujinuma, T. Maximov, Tree-ring analysis and modeling approaches yield contrary response of circumboreal forest productivity to climate change. *Glob. Chang. Biol.* **23**, 5179–5188 (2017).
13. S. Fatichi, S. Leuzinger, C. Körner, Moving beyond photosynthesis: From carbon source to sink-driven vegetation modeling. *New Phytol.* **201**, 1086–1095 (2014).
14. S. Sitch, P. Friedlingstein, N. Gruber, S. D. Jones, G. Murray-Tortarolo, A. Ahlstrom, S. C. Doney, H. Graven, C. Heinze, C. Huntingford, S. Levis, P. E. Levy, M. Lomas, B. Poulter, N. Viovy, S. Zaehle, N. Zeng, A. Arneth, B. Gordon, L. Bopp, J. G. Canadell, F. Chevallier, P. Ciais, R. Ellis, E. Gloor, P. Peylin, S. L. Piao, C. Le Quere, B. Smith, Z. Zhu, R. Mynen, Recent trends and drivers of regional sources and sinks of carbon dioxide. *Biogeosciences* **12**, 653–679 (2015).
15. W. R. L. Anderegg, C. Schwalm, F. Biondi, J. J. Camarero, G. Koch, M. Litvak, K. Ogle, J. D. Shaw, E. Shevliakova, A. P. Williams, A. Wolf, E. Ziaco, S. Pacala, Pervasive drought legacies in forest ecosystems and their implications for carbon cycle models. *Science* **349**, 528–532 (2015).
16. C. Pappas, M. D. Mahecha, D. C. Frank, F. Babst, D. Koutsoyiannis, Ecosystem functioning is enveloped by hydrometeorological variability. *Nat. Ecol. Evol.* **1**, 1263–1270 (2017).
17. M. Thurner, C. Beer, P. Ciais, A. D. Friend, A. Ito, A. Kleidon, M. R. Lomas, S. Quegan, T. T. Rademacher, S. Schaphoff, M. Tum, A. Wiltshire, N. Carvalhais, Evaluation of climate-related carbon turnover processes in global vegetation models for boreal and temperate forests. *Glob. Chang. Biol.* **23**, 3076–3091 (2017).
18. F. Babst, B. Poulter, V. Trouet, K. Tan, B. Neuwirth, R. Wilson, M. Carrer, M. Grabner, W. Tegel, T. Levanic, M. Panayotov, C. Urbinati, O. Bouriaud, P. Ciais, D. Frank, Site- and species-specific responses of forest growth to climate across the European continent. *Glob. Ecol. Biogeogr.* **22**, 706–717 (2013).
19. C. R. Rollinson, Y. Liu, A. Raiho, D. J. P. Moore, J. McLachlan, D. A. Bishop, A. Dye, J. H. Matthes, A. Hessl, T. Hickler, N. Pederson, B. Poulter, T. Quaife, K. Schaefer, J. Steinkamp, M. C. Dietze, Emergent climate and CO₂ sensitivities of net primary productivity in ecosystem models do not agree with empirical data in temperate forests of eastern North America. *Glob. Chang. Biol.* **23**, 2755–2767 (2017).
20. Z. Zhang, F. Babst, V. Bellassen, D. Frank, T. Launois, K. Tan, P. Ciais, B. Poulter, Converging climate sensitivities of European forests between observed radial tree growth and vegetation models. *Ecosystems* **21**, 410–425 (2017).
21. J. Guillemot, C. Francois, G. Hmimina, E. Dufrêne, N. K. Martin-StPaul, K. Soudani, G. Marie, J. M. Ourcival, N. Delpierre, Environmental control of carbon allocation matters for modelling forest growth. *New Phytol.* **214**, 180–193 (2017).
22. B. J. Frey, D. Dueck, Clustering by passing messages between data points. *Science* **315**, 972–976 (2007).
23. M. R. Osborne, Fisher's method of scoring. *Int. Stat. Rev.* **60**, 99–117 (1992).
24. H. D. Adams, M. J. B. Zeppel, W. R. L. Anderegg, H. Hartmann, S. M. Landhäusser, D. T. Tissue, T. E. Huxman, P. J. Hudson, T. E. Franz, C. D. Allen, L. D. L. Anderegg, G. A. Barron-Gafford, D. J. Beerling, D. D. Breshears, T. J. Brodribb, H. Bugmann, R. C. Cobb, A. D. Collins, L. T. Dickman, H. Duan, B. E. Ewers, L. Galiano, D. A. Galvez, N. Garcia-Forner, M. L. Gaylord, M. J. Germino, A. Gessler, U. G. Hacke, R. Hakamada, A. Hector, M. W. Jenkins, J. M. Kane, T. E. Kolb, D. J. Law, J. D. Lewis, J.-M. Limousin, D. M. Love, A. K. Macalady, J. Martínez-Vilalta, M. Mencuccini, P. J. Mitchell, J. D. Muss, M. J. O'Brien, A. P. O'Grady, R. E. Pangle, E. A. Pinkard, F. I. Piper, J. A. Plaut, W. T. Pockman, J. Quirk, K. Reinhardt, F. Ripullone, M. G. Ryan, A. Sala, S. Sevanto, J. S. Sperry, R. Vargas, M. Vennetier, D. A. Way, C. Xu, E. A. Yepez, N. G. McDowell, A multi-species synthesis of physiological mechanisms in drought-induced tree mortality. *Nat. Ecol. Evol.* **1**, 1285–1291 (2017).
25. P. S. A. Beck, G. P. Juday, C. Alix, V. A. Barber, S. E. Winslow, E. E. Sousa, P. Heiser, J. D. Herriges, S. J. Goetz, Changes in forest productivity across Alaska consistent with biome shift. *Ecol. Lett.* **14**, 373–379 (2011).
26. G. T. Pederson, S. T. Gray, C. A. Woodhouse, J. L. Betancourt, D. B. Fagre, J. S. Littell, E. Watson, B. H. Luckman, L. J. Graumlich, The unusual nature of recent snowpack declines in the North American cordillera. *Science* **333**, 332–335 (2011).
27. A. P. Williams, C. Xu, N. G. McDowell, Who is the new sheriff in town regulating boreal forest growth. *Environ. Res. Lett.* **6**, 041004 (2011).
28. G. P. Juday, C. Alix, T. A. Grant III, Spatial coherence and change of opposite white spruce temperature sensitivities on floodplains in Alaska confirms early stage boreal biome shift. *For. Ecol. Manage.* **350**, 46–61 (2015).
29. M. P. Girardin, E. H. Hogg, P. Y. Bernier, W. A. Kurz, X. Jing Guo, G. Cyr, Negative impacts of high temperatures on growth of black spruce forests intensify with the anticipated climate warming. *Glob. Chang. Biol.* **22**, 627–643 (2016).
30. S. Sevanto, N. G. Mcdowell, L. T. Dickman, R. Pangle, W. T. Pockman, How do trees die? A test of the hydraulic failure and carbon starvation hypotheses. *Plant Cell Environ.* **37**, 153–161 (2014).

31. R. A. Hember, W. A. Kurz, N. C. Coops, Relationships between individual-tree mortality and water-balance variables indicate positive trends in water stress-induced tree mortality across North America. *Glob. Chang. Biol.* **23**, 1691–1710 (2017).

32. Z. Zhu, R. B. Myneni, M. Huang, Z. Zeng, J. G. Canadell, P. Ciais, S. Sitch, P. Friedlingstein, A. Arneth, C. Cao, L. Cheng, E. Kato, C. Koven, Y. Li, X. Lian, Y. Liu, R. Liu, J. Mao, Y. Pan, S. Peng, J. Peñuelas, B. Poulter, T. A. M. Pugh, B. D. Stocker, N. Viovy, X. Wang, Y. Wang, Z. Xiao, H. Yang, S. Zaehle, N. Zeng, Greening of the Earth and its drivers. *Nat. Clim. Chang.* **6**, 791–795 (2016).

33. L. D'Orangeville, J. Maxwell, D. Kneeshaw, N. Pederson, L. Duchesne, T. Logan, D. Houle, D. Arseneault, C. M. Beier, D. A. Bishop, D. Druckenbrod, S. Fraver, F. Girard, J. Halman, C. Hansen, J. L. Hart, H. Hartmann, M. Kaye, D. Leblanc, S. Manzoni, R. Ouimet, S. Rayback, C. R. Rollinson, R. P. Phillips, Drought timing and local climate determine the sensitivity of eastern temperate forests to drought. *Glob. Chang. Biol.* **24**, 2339–2351 (2018).

34. C. Nehrbass-Ahles, F. Babst, S. Klesse, M. Nötzli, O. Bouriaud, R. Neukom, M. Dobbertin, D. Frank, The influence of sampling design on tree-ring-based quantification of forest growth. *Glob. Chang. Biol.* **20**, 2867–2885 (2014).

35. F. Babst, P. Bodesheim, N. Charney, A. D. Friend, M. P. Girardin, S. Klesse, D. J. P. Moore, K. Seftigen, J. Björklund, O. Bouriaud, A. Dawson, R. J. DeRose, M. C. Dietze, A. H. Eckes, B. Enquist, D. C. Frank, M. D. Mahecha, B. Poulter, M. E. K. Evans, When tree-rings go global: Challenges and opportunities of retro- and prospective insight. *Quat. Sci. Rev.* **197**, 1–20 (2018).

36. M. P. Girardin, O. Bouriaud, E. H. Hogg, W. Kurz, N. E. Zimmermann, J. M. Metsaranta, R. Jong, DC Frank, J. Esper, U Büntgen, X. J. Guo, J. Bhatti, No growth stimulation of Canada's boreal forest under half-century of combined warming and CO_2 fertilization. *Proc. Natl. Acad. Sci. U.S.A.* **113**, E8406–E8414 (2016).

37. S. Klesse, F. Babst, S. Lienert, R. Spahni, F. Joos, O. Bouriaud, M. Carrer, A. Di Filippo, B. Poulter, V. Trotsiuk, R. Wilson, D. C. Frank, A combined tree ring and vegetation model assessment of European forest growth sensitivity to interannual climate variability. *Global Biogeochem. Cycles* **32**, 1226–1240 (2018).

38. J. M. Housset, S. Nadeau, N. Isabel, C. Depardieu, I. Duschesne, P. Lenz, M. Girardin, Tree rings provide a new class of phenotypes for genetic associations that foster insights into adaptation of conifers to climate change. *New Phytol.* **218**, 630–645 (2018).

39. K. A. Novick, D. L. Ficklin, P. C. Stoy, C. A. Williams, G. Bohrer, A. C. Oishi, S. A. Papuga, P. D. Blanken, A. Noormets, B. N. Sulman, R. L. Scott, L. Wang, R. P. Phillips, The increasing importance of atmospheric demand for ecosystem water and carbon fluxes. *Nat. Clim. Chang.* **6**, 1023–1027 (2016).

40. J. S. Clark, L. Iverson, C. W. Woodall, C. D. Allen, D. M. Bell, D. C. Bragg, A. W. D'Amato, F. W. Davis, M. H. Hersh, I. Ibanez, S. T. Jackson, S. Matthews, N. Pederson, M. Peters, M. W. Schwartz, K. M. Waring, N. E. Zimmermann, The impacts of increasing drought on forest dynamics, structure, and biodiversity in the United States. *Glob. Chang. Biol.* **22**, 2329–2352 (2016).

41. I. Harris, P. D. Jones, T. J. Osborn, D. H. Lister, Updated high-resolution grids of monthly climatic observations – the CRU TS3.10 dataset. *Int. J. Climatol.* **34**, 623–642 (2014).

42. S. M. Vicente-Serrano, S. Beguería, J. I. López-Moreno, A multiscalar drought index sensitive to global warming: The standardized precipitation evapotranspiration index. *J. Climate* **23**, 1696–1718 (2010).

43. R. J. Hijmans, S. E. Cameron, J. L. Parra, P. G. Jones, A. Jarvis, Very high resolution interpolated climate surfaces for global land areas. *Int. J. Climatol.* **25**, 1965–1978 (2005).

Citation: F. Babst, O. Bouriaud, B. Poulter, V. Trouet, M. P. Girardin, D. C. Frank, Twentieth century redistribution in climatic drivers of global tree growth. *Sci. Adv.* **5**, eaat4313 (2019).

Science Advances

Twentieth century redistribution in climatic drivers of global tree growth

Flurin BabstOlivier BouriaudBenjamin PoulterValerie TrouetMartin P. GirardinDavid C. Frank

View the article online
https://www.science.org/doi/10.1126/sciadv.aat4313
Permissions
https://www.science.org/help/reprints-and-permissions

Use of this article is subject to the Terms of service